An iterative analytic–numerical method for scattering from a target buried beneath a rough surface*

Xu Run-Wen(徐润汶)†, Guo Li-Xin(郭立新), and Wang Rui(王 蕊)

School of Physics and Optoelectronic Engineering, Xidian University, Xi'an 710071, *China*

(Received 17 March 2014; revised manuscript received 15 April 2014; published online 17 September 2014)

An efficiently iterative analytical–numerical method is proposed for two-dimensional (2D) electromagnetic scattering from a perfectly electric conducting (PEC) target buried under a dielectric rough surface. The basic idea is to employ the Kirchhoff approximation (KA) to accelerate the boundary integral method (BIM). Below the rough surface, an iterative system is designed between the rough surface and the target. The KA is used to simulate the initial field on the rough surface based on the Fresnel theory, while the target is analyzed by the boundary integral method to obtain a precise result. The fields between the rough surface and the target can be linked by the boundary integral equations below the rough surface. The technique presented here is highly efficient in terms of computational memory, time, and versatility. Numerical simulations of two typical models are carried out to validate the method.

Keywords: boundary integral method (BIM), Kirchhoff approximation (KA), rough surface, target

PACS: 41.20.–q, 42.25.Bs, 42.25.Dd **DOI:** 10.1088/1674-1056/23/11/114101

1. Introduction

Modeling of scattering and radiation from a target buried below a rough ground is a subject of great interest in many applications, such as buried landmines, pipes, submarines, and other buried targets of interest beneath a rough surface. The method of moments (MoM)[1] was used to discuss the scattering from a partially buried perfectly electric conducting (PEC) cylinder at a dielectric rough interface. The electromagnetic scattering from a two-layered rough interface with a PEC object was studied by the MoM in Ref. [2]. An improved algorithm based on the MoM was proposed[3] to solve the scattering problem of cylindrical bodies buried beneath a rough surface. The steepest descent fast multipole method (SDFMM) was employed in Ref. [4] to study multiple objects buried under the ground. However, the numerical methods mentioned above are all based on the boundary integral method (BIM), so they consume a lot of computational memories and time when the rough surface has a large scale. To improve the algorithmic efficiency and reduce the computational memory, the small slope approximation (SSA) was applied in Ref. [5] to study the scattering from a time-varying Gerstners sea surface. In Ref. [6], Lawrence and Sarabandi solved the problem of a cylinder buried beneath a slightly rough surface based on the small perturbation method (SPM).[7] As an analytical method, the method in Ref. [6] is fast and efficient, however, it is just suitable for slightly rough surfaces. To combine advantages of analytical methods and numerical methods, the scattering from cylinders buried under a slightly rough surface was studied in Refs. [8] and [9] based on the cylindrical wave approach and the SPM. The propagation-inside-layer-expansion method (PILEM) combined with physical optics (PO) was used in Ref. [10] to analyze the scattering from an object below a dielectric rough surface. Based on the equivalent principles, a hybrid MoM–PO method[11] was applied to simulate scattering from a PEC target above a PEC rough surface. A novel hybrid FEM-high frequency technique[12] for the efficient analysis of general scattering and radiation problems was also presented. The boundary integral method combined with the Kirchhoff approximation (KA) was used in Ref. [13] to study the scattering properties of a PEC target above a PEC rough surface.

In this paper, an efficient hybrid iterative analytical–numerical algorithm is firstly designed for a two-dimensional (2D) model of an object buried beneath a dielectric rough surface. Inside the rough ground, the rough surface and the target form an iterated system, and the interactions between the two parts are taken into account by updating the field on the rough surface and the target. In Section 2, a general formulation of the iterative analytical–numerical method combining BIM with KA[14,15] is presented. Some numerical simulations are performed to validate our hybrid method in Section 3. Conclusions are summarized in Section 4. A time factor $e^{-i\omega t}$ is assumed and omitted throughout this paper.

2. Formulations and theories

Consider both the transverse magnetic (TM) polarization (where the electric field E only has a component along the z axis) and the transverse electric (TE) polarization (where the

*Project supported by the National Natural Science Foundation of China for Distinguished Young Scholars (Grant No. 61225002), the Fundamental Research Funds for the Central Universities, China (Grant No. K50510070001), and the National Natural Science Foundation of China (Grant No. 61301070).

†Corresponding author. E-mail: rwxu719@126.com

© 2014 Chinese Physical Society and IOP Publishing Ltd

magnetic field H only has a component along the z axis) 2D scattering problems, the incident wave impinges upon a PEC target with an arbitrary shape buried at a depth d beneath the rough surface. Figure 1 depicts a general schematic diagram of the scattering scenario. The axis of the target is parallel to the z axis. The whole space is separated into two-half spaces by the rough surface. Here $L_{\rm rs}$ is the length of the truncated rough surface, $\Gamma_{\rm S}$ denotes the profile of the truncated rough surface, and $\Gamma_{\rm O}$ is the boundary of the PEC target. The incident wave impinges upon the surface with an incident angle $\theta_{\rm inc}$ and is scattered with a scattering angle $\theta_{\rm scat}$. Vectors $\hat{\boldsymbol{n}}_{\rm s}$ and $\hat{\boldsymbol{n}}_{\rm o}$ are the unit normal vectors of the rough surface and the target, respectively. As shown in Fig. 1, two half regions $\Omega_{\rm U}$ and $\Omega_{\rm D}$ have permittivity and permeability given by ε_1, μ_1 and ε_2, μ_2, respectively.

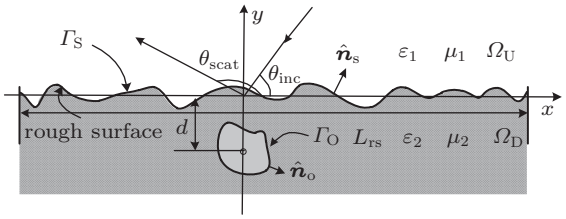


Fig. 1. The 2D scattering problem of a target buried beneath a rough surface.

The rough surface can be obtained by using the Monte Carlo method[16,17] based on the corresponding power spectrum function. Due to the infinite length of the rough surface, it needs to be truncated into a limited length in the simulation. This can introduce an artificial truncated effect at the ends of the rough surface. To reduce the artificial truncated effect, a tapered incident wave[18] is chosen as the incident source, which decreases to a very small value at the ends of the rough surface. The form of the incident wave can be expressed as

$$\begin{aligned}\Phi^{\rm inc}(\boldsymbol{r}) &= \exp[{\rm i}\boldsymbol{k}\cdot\boldsymbol{r}(1+w(\boldsymbol{r}))]\\ &\quad\times\exp\left[-(x-y\cot\theta_{\rm inc})^2/g^2\right],\end{aligned}\tag{1}$$

where $w(\boldsymbol{r}) = \left[2(x-y\cot\theta_{\rm inc})^2/g^2-1\right]/(kg\sin\theta_{\rm inc})^2$, $\boldsymbol{k}$ is the wavenumber in the space, g is the tapered factor, and $\boldsymbol{r}$ is the position vector.

Assume that the initial field on the rough surface and the target is zero. Firstly, the total field on the rough surface can be expressed by the following equations based on the KA:

$$\Phi(\boldsymbol{r})|_{\Gamma_{\rm S+}} = [1+R(\boldsymbol{r})]\,\Phi^{\rm inc}(\boldsymbol{r})\Big|_{\Gamma_{\rm S+}},\tag{2}$$

$$\frac{\partial\Phi(\boldsymbol{r})}{\partial n_{\rm s}}\bigg|_{\Gamma_{\rm S+}} = [1-R(\boldsymbol{r})]\,\frac{\partial\Phi^{\rm inc}(\boldsymbol{r})}{\partial n_{\rm s}}\bigg|_{\Gamma_{\rm S+}},\tag{3}$$

where $\Gamma_{\rm S+}$ denotes the side of a rough surface in air $\Omega_{\rm U}$. The Fresnel reflective coefficients for TM and TE cases on boundary $\Gamma_{\rm S+}$ are

$$R(\boldsymbol{r}) = \frac{\sqrt{\varepsilon_1}\cos\theta-\sqrt{\varepsilon_2}\cos\theta''}{\sqrt{\varepsilon_1}\cos\theta+\sqrt{\varepsilon_2}\cos\theta''},\quad \text{for TM case;}\tag{4}$$

$$R(\boldsymbol{r}) = \frac{\sin\theta\cos\theta-\sin\theta''\cos\theta''}{\sin\theta\cos\theta+\sin\theta''\cos\theta''},\quad \text{for TE case;}\tag{5}$$

where θ is the local incident angle on the rough surface, and θ'' is the local reflective angle on the rough surface. Based on Eqs. (1)–(5), the field on the rough surface can be obtained if we do not consider the influence of the target. On the boundary of the rough surface, the continuous conditions between domain $\Omega_{\rm U}$ and domain $\Omega_{\rm D}$ are

$$\Phi|_{\Gamma_{\rm S+}} = \Phi|_{\Gamma_{\rm S-}};\quad \frac{1}{\rho_+}\frac{\partial\Phi}{\partial n_{\rm s}}\bigg|_{\Gamma_{\rm S+}} = \frac{1}{\rho_-}\frac{\partial\Phi}{\partial n_{\rm s}}\bigg|_{\Gamma_{\rm S-}},\tag{6}$$

where $\rho=\mu_{\rm r}$ for the TM case, $\rho=\varepsilon_{\rm r}$ for the TE case, and $\Gamma_{\rm S-}$ represents the side of the rough surface inside ground $\Omega_{\rm D}$. If we neglect the impact of the target temporarily, the field in domain $\Omega_{\rm D}$ can be obtained by the following boundary integral equation (BIE):[16]

$$\begin{aligned}\Phi_{\rm D}(\boldsymbol{r}') &= -\int_{\Gamma_{\rm S-}}\left[\Phi(\boldsymbol{r})\frac{\partial G_2(\boldsymbol{r},\boldsymbol{r}')}{\partial n_{\rm s}}\right.\\ &\quad\left.-G_2(\boldsymbol{r},\boldsymbol{r}')\frac{\partial\Phi(\boldsymbol{r})}{\partial n_{\rm s}}\right]{\rm d}\Gamma,\end{aligned}\tag{7}$$

where $G_2(\boldsymbol{r},\boldsymbol{r}')$ is the Green function of space $\Omega_{\rm D}$.

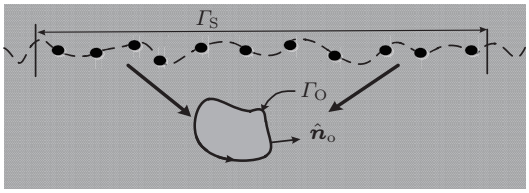


Fig. 2. The iterative approach for a target buried beneath a rough surface.

By neglecting the rough surface temporarily, the scattering model is built on the assumption that the target is buried in an infinite space filled by a medium with the same ε_2 and μ_2 as the dielectric rough surface. As shown in Fig. 2, the rough surface is replaced by many sources in every subsegment, and these sources can induce electromagnetic field $\phi^{\rm inc}$ on the target, which can be evaluated by Eq. (7). Based on the boundary integral method, an integral equation of the PEC target can be obtained as

$$\begin{aligned}\xi\Phi(\boldsymbol{r}') &= \phi^{\rm inc}(\boldsymbol{r}')+\int_{\Gamma_{\rm O}}\left[\xi\Phi(\boldsymbol{r})\frac{\partial G_2(\boldsymbol{r},\boldsymbol{r}')}{\partial n_{\rm o}}\right.\\ &\quad\left.-(1-\xi)\,G_2(\boldsymbol{r},\boldsymbol{r}')\frac{\partial\Phi(\boldsymbol{r})}{\partial n_{\rm o}}\right]{\rm d}\Gamma,\end{aligned}\tag{8}$$

where $\xi=0$ for the TM case, and $\xi=1$ for the TE case. By expanding the field with the pulse basis function $f_n(\boldsymbol{r}')$ and adopting the point matching algorithm, the following weak form of Eq. (8) can be obtained in matrix notation:

$$\xi[\boldsymbol{A}][\boldsymbol{\Phi}]+(1-\xi)[\boldsymbol{B}][\boldsymbol{U}]=[\boldsymbol{b}],\tag{9}$$

where matrices $[\boldsymbol{\Phi}]$ and $[\boldsymbol{U}]$ represent $\Phi(\boldsymbol{r})$ and $\partial\Phi(\boldsymbol{r})/\partial n$ on the element of the object, respectively. The elements of matrices $[\boldsymbol{A}]$, $[\boldsymbol{B}]$, and $[\boldsymbol{b}]$ are

$$A_{ij} = f_i\left(\boldsymbol{r}_i'\right) - \int_{\boldsymbol{r}_j-\Delta l/2}^{\boldsymbol{r}_j+\Delta l/2} f_j\left(\boldsymbol{r}_j'\right)\frac{\partial G_2(\boldsymbol{r},\boldsymbol{r}_i')}{\partial n_{\rm o}}\,{\rm d}l, \quad (10)$$

$$B_{ij} = \int_{\boldsymbol{r}_j-\Delta l/2}^{\boldsymbol{r}_j+\Delta l/2} f_j\left(\boldsymbol{r}_j'\right)\frac{\partial G_2(\boldsymbol{r},\boldsymbol{r}_i')}{\partial n_{\rm o}}\,{\rm d}l, \quad (11)$$

$$b_i = \phi^{\rm inc}\left(\boldsymbol{r}_i'\right). \quad (12)$$

The above matrix equation (9) can be solved based on the conjugated gradient method (CGM). Because only the target is solved by the boundary integral equation in our iterated method, this hybrid method is more efficient than the traditional MoM.

In the next step, the scattering field induced by the target on the rough surface can be expressed as

$$\Phi_{\rm O\to S}^{\rm scat}\left(\boldsymbol{r}'\right) = \int_{\Gamma_{\rm O}}\left[\xi\Phi(\boldsymbol{r})\frac{\partial G_2(\boldsymbol{r},\boldsymbol{r}')}{\partial n_{\rm o}} - (1-\xi)G_2(\boldsymbol{r},\boldsymbol{r}')\frac{\partial\Phi(\boldsymbol{r})}{\partial n_{\rm o}}\right]{\rm d}\Gamma. \quad (13)$$

Because $\varepsilon_2 > \varepsilon_1$, the phenomenon of total reflection occurs at interface $\Gamma_{\rm S-}$ of the rough surface when $\sin\theta > \sqrt{\varepsilon_1/\varepsilon_2}$. However, the forms of the Fresnel reflective coefficients are still satisfied when the following substitutions are made:

$$\sin\theta'' \to \frac{\sin\theta}{n_{12}};\quad \cos\theta'' \to {\rm i}\sqrt{\frac{\sin^2\theta}{n_{12}^2}-1};\quad n_{12} = \sqrt{\frac{\varepsilon_1}{\varepsilon_2}}. \quad (14)$$

The total field on boundary $\Gamma_{\rm S-}$ can be obtained based on Eqs. (13) and (14). Then the iteration goes on to the step of solving Eq. (7), and continues the circulation until the field on the target and the rough surface reaches convergence. The algorithmic convergence can be judged by the following equation:

$$\left|\sum_{i=1}^{n}\Phi_i^{k+1} - \sum_{i=1}^{n}\Phi_i^{k}\right| \Big/ \sum_{i=1}^{n}\Phi_i^{k} = \gamma, \quad (15)$$

where Φ is the field on the rough surface and the target in each iteration step, i denotes the nodes on the model, and k is the iteration time. Symbol γ denotes the iterated error, and the iteration can be considered to reach convergence when it is less than 10^{-3}. When the iteration above is finished, the total field and its normal derivation on boundary $\Gamma_{\rm S-}$ and the target are obtained. Then the field information $\Phi|_{\Gamma_{\rm S+}}$ and $\partial\Phi/\partial n|_{\Gamma_{\rm S+}}$ in the air can be obtained based on Eq. (6).

This iterative analytical–numerical method is based on the Kirchhoff approximation and the boundary integral method. For the scattering model of a target buried beneath a rough surface, the KA is used to simulate the scattering from the rough surface based on the Fresnel theory. On the other hand, the precise simulation of the target is expressed by the boundary integral method. The interaction between the rough surface and the target is taken into account by an iterative algorithm. The iterative algorithm is a powerful electromagnetic simulation tool, which combines the numerical method with the analytical method based on an integral based approach. It is worthwhile noting that the rough surface should satisfy the KA conditions of $k_0 l > 6$ and $l^2 > 2.76\delta\lambda$ in the TM and the TE cases, and the medium permittivity has a little effect on the precision of the iterative method.

3. Numerical examples

Several numerical simulations are considered to demonstrate the general solutions derived above and to illustrate the accuracy and effectiveness of our proposed method. In our simulations, the length of the truncated rough surface is $L_{\rm rs} = 102.4\lambda$, λ is the wavelength of the incident wave, the tapered factor of the incident wave is $g = L_{\rm rs}/4.0$, and the permeability in all regions is $\mu_1 = \mu_2 = \mu_0$. The first example of a PEC circular cylinder buried beneath a rough ground is devoted to the validation of the proposed method. The rough ground is the Gaussian rough surface, whose spectrum can be generated by the Gaussian power spectrum function

$$S(k) = \frac{\delta^2 l}{2\sqrt{\pi}}\exp(-k^2l^2/4), \quad (16)$$

where δ denotes the root mean square height, and l represents the correlative length.

Figures 3(a) and 3(b) give the iterated error γ versus the iterated step n for the circular cylinder buried beneath the rough ground with different parameters. The incident angle is $\theta_{\rm inc} = \pi/2$. The object is assumed to be a cylinder with radius $r = 1.0\lambda$ at a buried depth $d = 2.0\lambda$. The ground is a Gaussian rough surface with $\delta = 0.1\lambda$ and $l = 2.0\lambda$, and the relative permittivity of the rough surface is $\varepsilon_{\rm r2} = (2.0, 0.1)$ by default. In Figs. 3(a) and 3(b), case 1 shows the result of the default model; case 2 shows the result of a rough surface with $\delta = 0.3\lambda$ and $l = 1.5\lambda$; case 3 shows the result of a target with $r = 1.5\lambda$ at a buried depth $d = 3.0\lambda$; case 4 shows the result of a dielectric rough surface with $\varepsilon_{\rm r2} = (2.5, 0.3)$. In each iteration of the hybrid algorithm, the CGM is used to numerically solve the BIE, and the iterative loop of the CGM is called the inner loop. The tolerance error of two inner iterative steps is set at $\gamma < 10^{-3}$. As shown in Figs. 3(a) and 3(b), the iterated error of the CGM decreases quickly with increasing the step of the iterative KA–BIM.

Comparisons of the solving time and the number of unknowns for different methods are shown in Table 1. The codes

are executed by a computer with a 2.50 GHz processor (Intel (R) Core (TM)2 Quad CPU), 3.47 GB memory, and Visual Fortran 6.5 compiler. In the application of KA–BIM, the number of unknowns is reduced to 5.7% of that in MoM for both TM and TE cases. As a result, the time consumption of KA–MoM decreases greatly in the treatment of the impedance matrix.

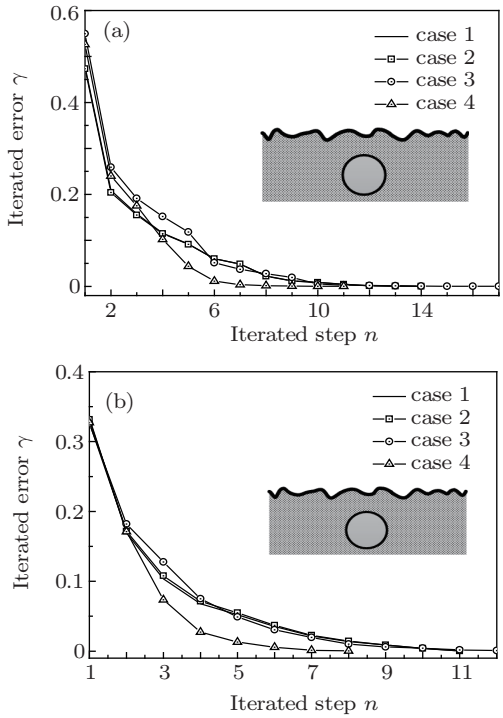


Fig. 3. Iterated error versus iterated step: (a) TM case, and (b) TE case.

Table 1. Time used and number of unknowns in MoM and KA–BIM.

Polarization	Method	Number of unknowns	Time used/ms
TM	MoM	2172	87670.8
	KA–BIM	125	48.9
TE	MoM	2172	39580.2
	KA–BIM	125	40.7

Figures 4(a) and 4(b) show the field information along the surface of the circular cylinder in the TM case and the TE case. The solutions obtained from MoM refers to using the MoM for the whole structure (including the rough surface and the object) to obtain the exact results. For the TM case, the total electric field on the PEC cylinder does not exist, and the normal derivation of the magnetic field is zero for the TE case. It can be seen that the two methods are almost perfectly matched for both TM and TE cases.

Figures 5(a) and 5(b) show the field information along the surface of the Gaussian rough surface in the TM case and the TE case in the air. The real and the imaginary parts of the total electric field on the rough surface in the TM case are plotted in Fig. 5(a), while the normal derivation of the total magnetic field on the rough surface in the TE case is plotted in Fig. 5(b).

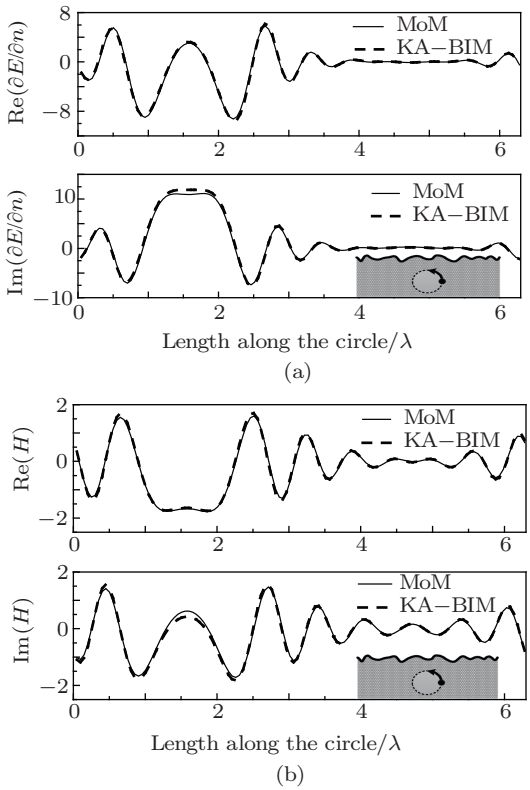


Fig. 4. The field information along the circular cylinder: (a) TM case, and (b) TE case.

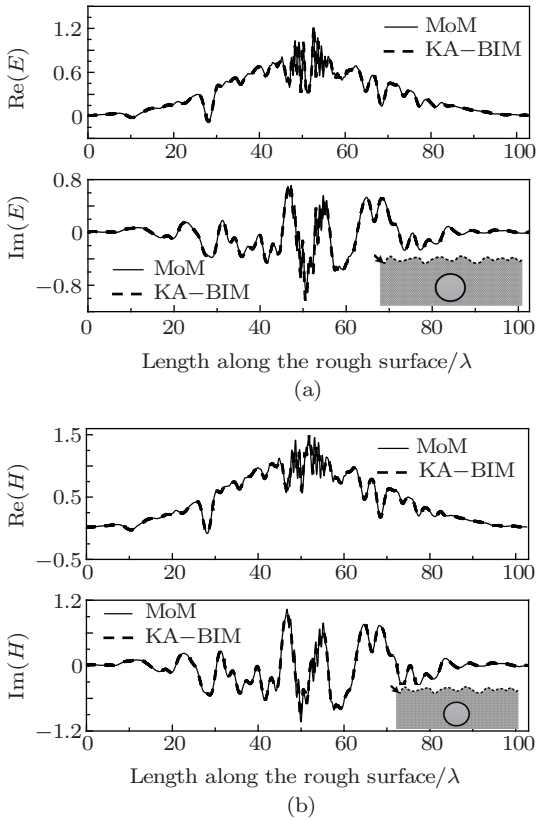


Fig. 5. The total field along the Gaussian rough surface: (a) TM case, and (b) TE case.

The well agreement shown in these figures validates the code of the hybrid method. To verify versatile applications of our method, the scattering from a PEC square cylinder buried beneath an exponentially correlated rough surface is considered in the next example, whose power spectrum function is given by

$$S(k) = \frac{\delta^2 l}{\pi(1+k^2l^2)}. \tag{17}$$

In Figs. 6(a) and 6(b), we give the results of the iterated error γ versus the iterated step n for the PEC square cylinder buried beneath the rough ground with different parameters. The default parameters of the model are set as follows. The incident angle is $\theta_{\rm inc} = \pi/3$, the depth of the square cylinder is $d = 4.0\lambda$, the length of the square cylinder is $l_{\rm s} = 2.0\lambda$, the root mean square height is $\delta = 0.2\lambda$, the correlative length is $l = 1.0\lambda$, and the permittivity ε_2 of the rough surface is $\varepsilon_{\rm r2} = (4.0, 0.2)$. In Figs. 6(a) and 6(b), case 1 shows the result of the default model; case 2 shows the result of a rough surface with $\delta = 0.5\lambda$ and $l = 2.0\lambda$; case 3 shows the result of a target with $r = 3.0\lambda$ at a buried depth $d = 5.0\lambda$; case 4 shows the result of a dielectric ground with $\varepsilon_{\rm r2} = (6.0, 0.4)$. As shown in Figs. 6(a) and 6(b), the convergence of the CGM in our hybrid method is very good.

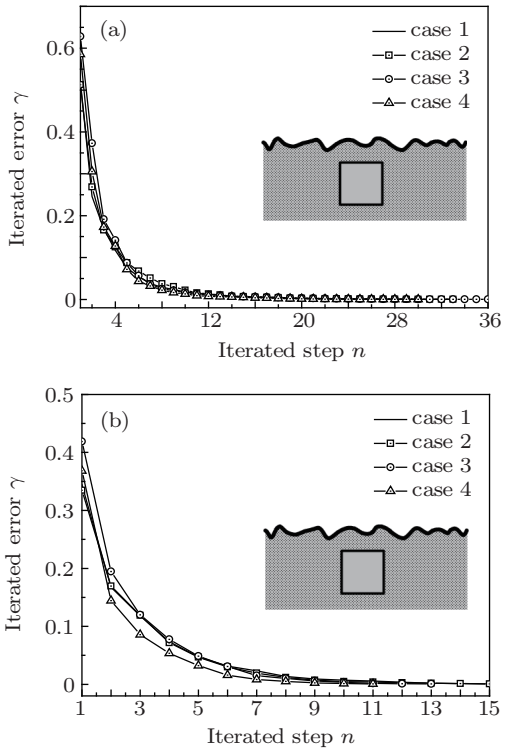


Fig. 6. Iterated error γ versus iterated step n: (a) TM case, and (b) TE case.

Comparisons of the simulation time and the number of unknowns using MoM and KA–BIM are shown in Table 2. The number of unknowns of KA–BIM is 6.7% of that in MoM for both polarizations, and the computational time using KA–BIM is very short compared with that of MoM.

Table 2. Time used and number of unknowns in MoM and KA–BIM.

Polarization	Method	Number of unknowns	Time used/ms
TM	MoM	2363	371054.1
	KA–BIM	158	109.7
TE	MoM	2363	237633.7
	KA–BIM	158	55.4

To show comparisons of the field inside the soil, we consider the distribution of the field along the surface of the target in Fig. 7. For the TM case, the total electric field on the PEC cylinder does not exist, and the normal derivation of the magnetic field is zero for the TE case. Obviously, the numerical results in the simulation are in good agreement with each other.

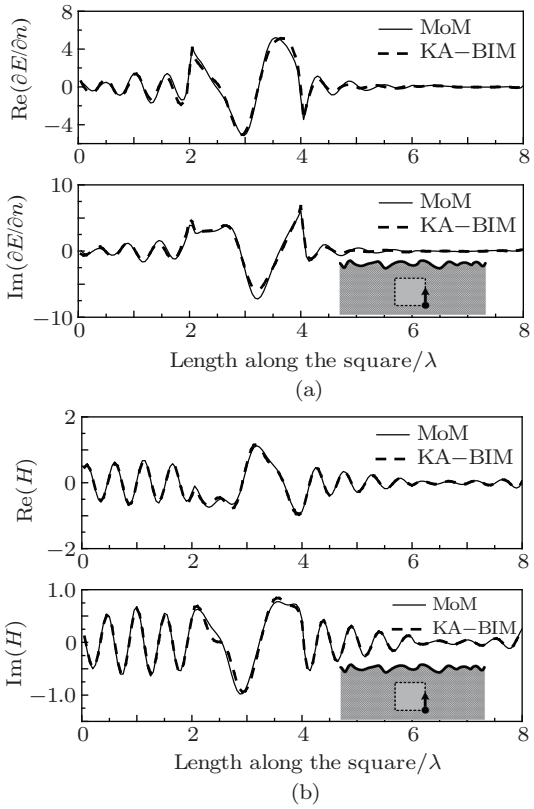


Fig. 7. The field information along the square cylinder: : (a) TM case, and (b) TE case.

Figure 8 shows the total field along the surface of the exponentially correlated rough surface under TM case and TE case in the air. The real and the imaginary parts of the total electric field on the rough surface are plotted in Fig. 8(a) for the TM case, and the magnetic field on the rough surface for the TE case is plotted in Fig. 8(b). It can be seen from Fig. 8 that all results from the hybrid method have good agreement with the MoM results, demonstrating the accuracy of the algorithm.

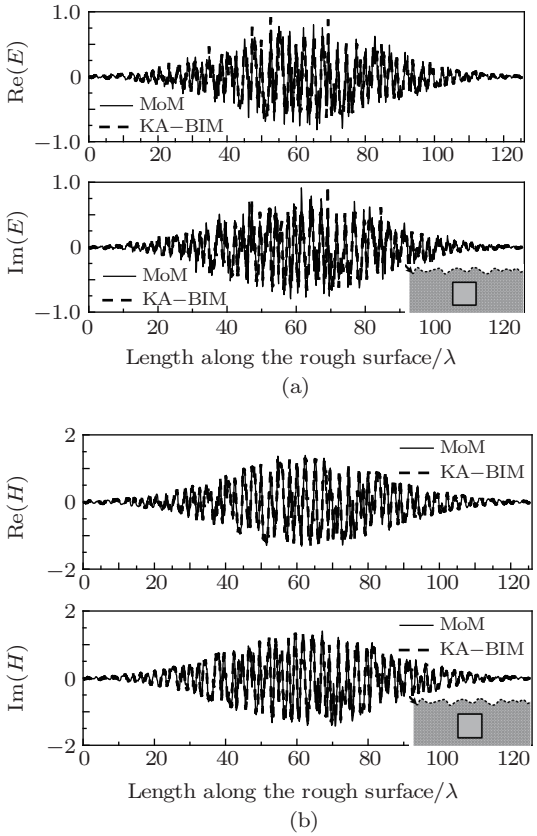


Fig. 8. The total field along the exponential rough surface: (a) TM case, and (b) TE case.

4. Conclusion

In this paper, an iterative analytical–numerical method is designed for electromagnetic scattering from a PEC target buried beneath a dielectric rough surface. In the iterative algorithm, the initial field on the rough surface is firstly estimated by the KA. Based on the boundary continuity conditions, the field information on the ventral of the rough surface can be obtained. By considering the interactions between the rough surface and the object, the scattering from the object is depicted by the BIM. When the fields on the target and the rough surface reach convergence, the precise results about the scattering model can be obtained. Compared with the literature, this work provides a novel iterative system below the rough surface based on the KA to accelerate the BIM. Our code shows good agreement and achieves high efficiency compared with the MoM. The iterative method can be used for the fast and efficient scattering simulation of a target buried under a large scale rough surface. If combining KA–BIM with the parallel technology or the fast algorithm of the BIM, the hybrid method can be expected to be more efficient. Future works on this topic include the improvement of the algorithmic precision, the application of this method to study a buried dielectric target under a rough surface, and the accelerated treatments on the method.

References

[1] Wang X, Gan Y B and Li L W 2003 *IEEE Antennas Wireless Propag. Lett.* **2** 319
[2] Wang A Q, Guo L X and Chai C 2011 *Chin. Phys. B* **20** 050201
[3] Altuncu Y, Yapar A and Akduman I 2006 *IEEE Trans. Geosci. Remote Sensing* **44** 1435
[4] El-Shenawee M 2003 *IEEE Trans. Antennas Propag.* **51** 802
[5] Zhang Y M, Wang Y H and Guo L X 2010 *Chin. Phys. B* **19** 054103
[6] Lawrence D E and Sarabandi K 2002 *IEEE Trans. Antennas Propag.* **50** 1368
[7] Ren X C and Guo L X 2008 *Chin. Phys. B* **17** 2491
[8] Fiaz M A, Frezza F, Pajewski L, Ponti C and Schettini G 2012 *IEEE Trans. Antennas Propag.* **60** 2834
[9] Fiaz M A, Frezza F, Pajewski L, Ponti C and Schettini G 2013 *Near Surface Geophysics* **11** 177
[10] Bourlier C, Pinel N and Kubické G 2013 *J. Opt. Soc. Am. A* **30** 1727
[11] He S Y and Zhu G Q 2007 *Microwave Opt. Tech. Lett.* **49** 2957
[12] García-Castillo L E, Gómez-Revuelto I and Sáez de Adana F 2005 *Computer Methods in Applied Mechanics and Engineering* **194** 637
[13] Ye H X and Jin Y Q 2007 *IEEE Trans. Geosci. Remote Sensing* **45** 1174
[14] Luo W, Zhang M, Zhou P and Yin H C 2010 *Chin. Phys. B* **19** 084102
[15] Nie D and Zhang M 2010 *Chin. Phys. B* **19** 074101
[16] Tsang L, Kong J A and Ding K H 2001 *Scattering of Electromagnetic Waves: Numerical Simulations*. (New York: Wiley Interscience) p. 124
[17] Wu Z S, Wang Y H and Guo L X 2005 *Chin. Phys. Lett.* **22** 2808
[18] Thorsos E I 1988 *J. Acoust. Soc. Am.* **83** 78